Available on CMS information server

CMS NOTE 1999/013

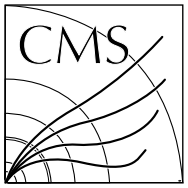

The Compact Muon Solenoid Experiment

CMS Note

Mailing address: CMS CERN, CH-1211 GENEVA 23, Switzerland

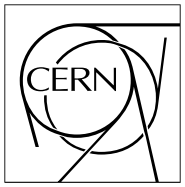

24 Feb. 1999

Signal-to-noise simulation of n^+ on n type Si micro-strip detectors

A. Bader, M. de Palma, S. My, V. Radicci, G. Raso, P. Tempesta

INFN and University of Bari, Bari, Italy

Abstract

Using a SPICE network model, we simulated the signal and noise of AC-coupled, single-sided, n^+ on n type Si micro-strip detectors connected to PreMux-128 read-out electronics. The detector response was studied before and after neutron irradiation with a fluence of $8.3 \cdot 10^{13}\ n/cm^2$. We compared the simulated and experimental signal-to-noise ratios.

1 Introduction

The signal-to-noise ratio (S/N) is the key parameter of Si micro-strip detectors to determine the detector efficiency. The general requirement to achieve good tracking capability in CMS experiment for LHC at CERN is $S/N > 10$ [1]. This performance should be maintained over 10 years of operation, by the time the fluence at the hottest part of the system is expected to reach about $1.6 \cdot 10^{14}$ n/cm^2.

The main component of the noise associated to the measurement of the charge signal in a Si detector is due to the front-end electronics. For a charge sensitive preamplifier, having CMOS input transistor, this noise, expressed it in Equivalent Noise Charge (ENC) units, is a linear function of the load capacitance seen by the preamplifier. After heavy irradiation the leakage current increases and gives a significant contribution to the total noise. Furthermore, due to the increasing number of trapping and recombination centers the charge collection efficiency decreases. This can be partly compensated by increasing the bias voltage. To keep the signal-to-noise ratio above the design value, it is necessary to operate the detector at high bias voltage and to cool the system below 0 $^\circ C$ (in CMS $T \simeq -10^\circ C$ and $V_{bias} \simeq 500$ V will be required by the end of the life-time of the detectors).

Both the signal amplitude and the noise level due to the detectors and the read-out electronics depend strongly on the capacitive coupling between the detector elements. In a detector that is AC coupled to the read-out electronics, the charge induced on an implant strip is shared among the coupling capacitance to the read-out electronics and other parasitic capacitances such as inter-strip and body capacitance. The charge coupling depends also on resistance parameters, for instance strip and bias resistance, inter-strip and strip-to-back resistance. Therefore, a careful analysis and simulation of capacitive and resistive coupling is essential in order to evaluate the signal-to-noise ratio.

In a previous work, we measured the main characteristics of n^+ on n type detectors before and after neutron irradiation and we implemented a SPICE network model for this detectors [2]. That model was very successful to simulate the frequency dependence of the capacitance measurements. Using the same model in this paper, we investigate the signal processing and signal-to-noise ratio and compare the results with the experimental data.

2 Detector Model

We studied single-sided, AC coupled, n^+ on n type SINTEF detectors. The detectors were 280 μm thick, the length of the strips was 57.4 mm. The number of the n^+ implant strips was 1025 with a pitch of 56 μm. The number of the metal strips was 512, so that every second n^+ implant strip only was read-out (112 μm read-out pitch). The intermediate strips did not have metal strips and we will refer to them as non-read-out strips. The isolation of the n^+ strips was achieved by using p^+ blocking strips. A detailed description and the main detector parameters can be found in ref. [2,3].

We studied the detector performance before irradiation and after neutron irradiation at a fluence of $8.3 \cdot 10^{13}$ n/cm^2. At this fluence the detectors were type inverted. The detectors were simulated using Powerview simulation software [4].

Our SPICE model is a network of resistors, capacitors and diodes containing more than 30000 circuit elements [2]. All capacitive and resistive couplings between the detector elements (e. g. read-out metal strips, n^+ implant, p^+ blocking strips, backplane) and strip resistance were taken into account. The $p-n$ junction was simulated with diodes. In our previous work we investigated two models: a simple one which did not contain the p^+ blocking strips (accounted only for the direct coupling between the n^+ implants) and an extended one which included also the coupling to the p^+ blocking strips. For non-irradiated detectors the two models resulted to be equivalent, while for irradiated detectors we obtained a better agreement with the measured values using the extended model. To simulate the signal processing and the noise we used this extended model. The parameter values were determined by direct measurements or, in a few cases, by simulating the capacitance measurements [2]. Table 1 shows the parameter values used in the models.

The test-beam results were obtained for two detectors connected together, which corresponds to a total strip length of 114.8 mm [5], while our simulation was done for a single detector (57.4 mm strip length). In a small region of the detector only every second read-out strip was connected to the read-out electronics, resulting in an effective read-out pitch of 224 μm. To simulate the signal processing and noise of a daisy-chained detector pair we simply multiplied the parameter values obtained for a single detector by

	Before irradiation		After irradiation	
	without p^+ stops	with p^+ stops	without p^+ stops	with p^+ stops
R_{bias}	$2\,M\Omega$	$2\,M\Omega$	$2\,M\Omega$	$2\,M\Omega$
R_n	$37\,K\Omega$	$37\,K\Omega$	$37\,K\Omega$	$37\,K\Omega$
R_m	$300\,\Omega$	$300\,\Omega$	$300\,\Omega$	$300\,\Omega$
R_{nm}	$5\,T\Omega$	$5\,T\Omega$	$500\,G\Omega$	$500\,G\Omega$
R_{nn}	$12\,G\Omega$	$13.8\,G\Omega$	$20\,M\Omega$	$23\,M\Omega$
R_p	∞	$592\,K\Omega$	∞	$592\,K\Omega$
R_{np}	∞	$48\,G\Omega$	∞	$80\,M\Omega$
I_{strip}	$200\ pA$	$200\ pA$	$900\ nA$	$900\ nA$
C_{AC}	$155\,pF$	$155\,pF$	$155\,pF$	$155\,pF$
C_{nn}	$6.66\,pF$	$1\,pF$	$3.6\,pF$	$1\,pF$
C_{nn+1}	$0.55\,pF$	$0.55\,pF$	$0.63\,pF$	$0.65\,pF$
C_{mm}	0	0	$0.2\,pF$	$0.5\,pF$
C_{nb}	$2.23\,pF$	$1.2\,pF$	$2.23\,pF$	$1.2\,pF$
C_{np}	0	$11.9\,pF$	0	$5.2\,pF$
C_{pb}	0	$1.8\,pF$	0	$1.8\,pF$

Table 1: The resistance and capacitance parameters used in the two network models. (m: metal strips, n: n^+ implants, p: p^+ blocking strips, $n+1$: second neighbour n^+ implants, b: backplane.)

2 or 0.5 depending on whether the elements are connected in series or in parallel (for example, the factor is 2 for the strip resistance and inter-strip capacitance, 0.5 for the inter-strip resistance).

3 Signal simulation

A particle crossing the detector may induce signals on one or more implant strips. In the case of 112 μm read-out pitch, we investigated two extreme cases: when the particles cross the detector close to a read-out or a non-read-out strip. The signal simulation consists of three steps: (i) charge generation on an implant strip associated with a crossing particle, (ii) evaluation of the induced signal on the metal strips (at the amplifier input) and (iii) processing of the signal through the preamplifier.

(i) In our model, we injected directly in the implant strip a signal of 22400 e^-, which corresponds to a minimum ionising particle (MIP) crossing a 280 μm thick detector. We approximated the signal shape of a MIP with simple broken lines (see in figure 1). The sharp peak of the first few ns is induced by the electrons, while the long tail can be associated with the holes, whose mobility is lower [6]. The effective shape of the signal is not critical in our simulation since the duration of the signal is shorter than 50 ns, the shaping time of the read-out electronics. The signal was injected at the opposite end of the implant strip with respect to the read-out electronics.

(ii) The signal and its integral (the total charge) were evaluated on the metal strips coupled to the implant strip. In the case of read-out strips, most of the charge is induced on a single strip. In the case of non-read-out strips we added the signals induced on the two neighbouring metal strips. The signals induced on further strips were low and they were not considered. Figure 1 compares the signal and the total charge injected into an implant strip (input signal) with the signal and charge induced on the metal strips.

The efficiency of the charge coupling is the ratio of the input and induced charge (see figure 1b). In table 2, we listed the efficiency of the charge coupling in the case of 112 μm read-out pitch, 57.4 mm and 114.8 mm strip length, before and after irradiation, and for read-out and non-read-out strips.

For comparison, we also calculated the charge coupling efficiency values using equations of ref. [7], which can be obtained by taking into account the charge sharing among the capacitances in the detector. For read-out strips

$$E_{nf} = \frac{C_{AC}}{C_{AC} + C_{nb} + 2(C'_{nn} + C_{nn+1})}, \tag{1}$$

where

a)

b)

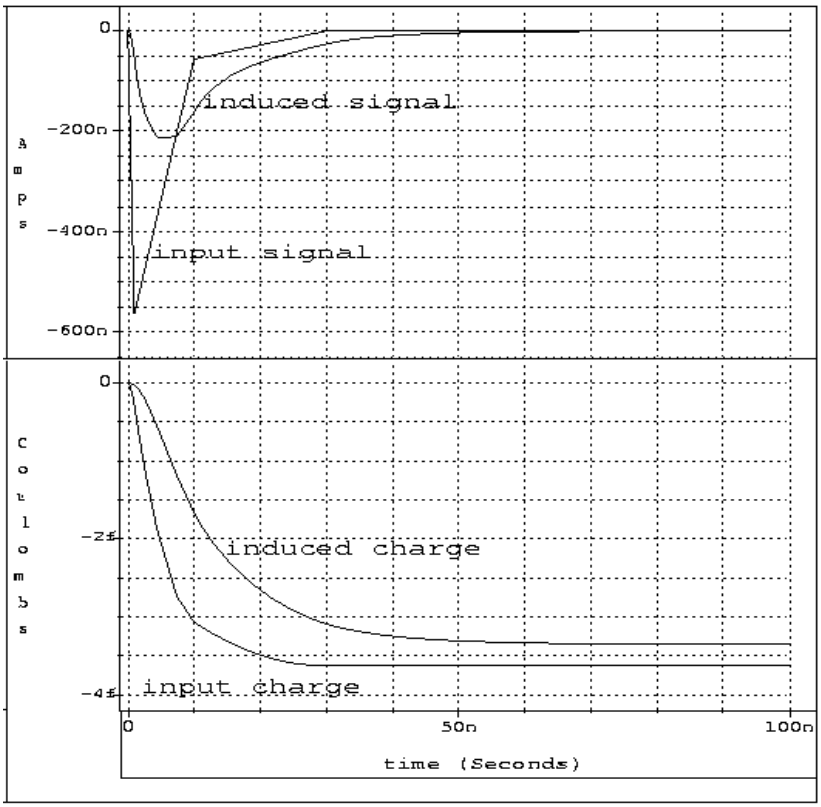

Figure 1: The signal (a) and charge (b) injected in an implant strip compared with the signal and charge induced on the closest metal strip in the case of read-out strip, before irradiation. (114.8 mm strip length)

$$C_{nn}^{'} = \frac{C_{nb} + C_{nn} + C_{nn+1}^{'}}{C_{nb} + 2C_{nn} + C_{nn+1}^{'}} C_{nn}, \quad C_{nn+1}^{'} = \frac{C_{nb} + C_{nn}}{C_{nb} + 2C_{nn} + C_{nn+1}} C_{nn+1}, \tag{2}$$

and for non-read-out strips

$$E_f = \frac{2C_{nn}C_{AC}}{C_{nb}(C_{nn} + C_{AC}) + 2C_{nn}C_{AC}}. \tag{3}$$

In these formulas C_{AC} is the coupling capacitance, C_{nn} is the inter-strip capacitance, C_{nn+1} is the second neighbour inter-strip capacitance and C_{nb} is the body capacitance. The couplings to further strips were not considered. Since these formulas refer to our simple model which did not contain the p^+ stops we used the corresponding parameter values (first and third columns of table 1).

While the calculation takes into account only the charge sharing among the capacitances of the detector elements, the SPICE model includes the resistive couplings, as well. In this latter case, the detector can be considered as a network of many RC-CR filters. Comparing the calculated and simulated values in table 2 one can see that the filtering of the signal is more significant when the charge is released on a non-read-out strip with respect to the case when it is induced on read-out strips. This effect reduces the collected charge.

The results show that the charge coupling is about 15-35 % lower when the signal is applied to a non-read-out strip. This is because the non-read-out strips are coupled to read-out electronics through inter-strip capacitance whose value is much lower than that of the coupling capacitance. Moreover, the inter-strip capacitance decreases with the irradiation (see table 2), as a consequence, the charge coupling efficiency drops by about 15-20 % after irradiation. This effect cannot be observed in the case of read-out strips, since they are directly coupled to the preamplifier through the coupling capacitance, which does not change with irradiation. As far as the charge collection efficiencies are concerned, the performances of the short (57.4 mm strip length) and the long (114.8 mm strip length) detector modules are very similar.

	57.4 mm strip length				114.8 mm strip length			
	Before irradiation		After irradiation		Before irradiation		After irradiation	
	read-out	non-read-out	read-out	non-read-out	read-out	non-read-out	read-out	non-read-out
Calc.	0.93	0.85	0.95	0.76	0.93	0.85	0.95	0.76
Sim.	0.92	0.77	0.94	0.62	0.91	0.73	0.93	0.62

Table 2: Calculated and simulated charge coupling efficiencies in the case of 57.4 mm and 114.8 mm long strips, before and after irradiation, for read-out and non-read-out strips (112 μm read-out pitch).

In the case of 224 μm read-out pitch the signal coupling efficiency is very low if the signal is induced on a non-read-out or not connected read-out strip, see table 3.

Before irradiation			After irradiation		
conn. read-out	non-read-out	not conn. read-out	conn. read-out	non-read-out	not conn. read-out
0.93	0.59	0.51	0.94	0.47	0.41

Table 3: Simulated charge coupling efficiency in the case of 114.8 mm strip length, before and after irradiation, for 224 μm read-out pitch.

(iii) In order to investigate the signal processing through the read-out chip we used the circuit model of PreMux-128 described in ref. [8]. This model consists of four modules: preamplifier, shaper, charge follower and output buffer. The preamplifier output level is proportional to the input charge, nominally 5 mV for 24000 electrons. The shaper forms a signal with fixed peaking time. The signal at the end of the buffer peaks at 50 ns, with an amplitude proportional to the input charge. This means that the signal amplitude measured at the output of the read-out electronics is proportional to the charge coupling efficiency. In the simulation the amplitude of the output signal, e. g. the amplification, can be modified by changing the output resistance value. In order to compare the signal amplitudes and the noise levels, we used always the same amplification.

Our model does not take into account the charge loss due to the recombination and trapping centers. This effect reduces the charge collection efficiency by approximately 5-10 % after irradiation at this fluence [9], which should be taken into account when comparing the simulated or calculated values with the experimental data.

4 Noise simulation

The main noise sources in AC coupled Si detectors are the following [7]:

1. The noise of the preamplifier, which is proportional to the input capacitive load:

$$ENC_1 = aC_{load} + b, \tag{4}$$

where C_{load} is the load capacitance in pF. For PreMux-128 $a = 41.5$ and $b = 558$ [8]. C_{load} can be calculated from

$$\frac{1}{C_{load}} = \frac{1}{C_{AC}} + \frac{1}{C_{nb} + 2(C'_{nn} + C_{nn+1})}. \tag{5}$$

2. The shot noise of the strip leakage current, which is significant after irradiation and can be calculated by:

$$ENC_2 = \frac{e}{2}\sqrt{\tau I_{strip}/q_e}, \tag{6}$$

where e is the Euler-constant, q_e is the electron charge, I_{strip} is the strip leakage current and τ is the shaping time.

3. The thermal noise of the bias resistor, R_{bias}, which can be calculated by:

$$ENC_3 = \frac{e}{q_e}\sqrt{\tau kT/2R_{bias}}. \tag{7}$$

4. The thermal noise of the series resistors:

$$ENC_4 = \frac{e}{q_e}C_{load}\sqrt{kTR_s/2\tau}, \tag{8}$$

where R_s is an effective series resistance, which is about one third of the metal strip resistance [7].

The total noise can be obtained by adding in quadrature all noise components:

$$ENC^2 = ENC_1^2 + ENC_2^2 + ENC_3^2 + ENC_4^2 \tag{9}$$

The noise components 1 and 4 are considered "series noise" since they can be modeled by a noise voltage generator connected in series to the read-out electronics. The noise components 2 and 3 are called "parallel noise" components and can be modelled by noise current generators connected in parallel to the read-out electronics.

We have simulated the noise performance of our system using SPICE. The noise components 3 and 4 are automatically taken into account since the bias and strip resistors were directly included in the SPICE model.

To simulate the noise of the preamplifier (noise component 1) we used the circuit model of the read-out electronics described in [8], which contains a MOSFET input transistor. The parameters of this transistor were tuned to have the noise characteristics described by equation (4).

To simulate the noise due to the leakage current, we replaced the body capacitors and resistors with diodes in our detector model described in [2]. The parameters of the diodes were set to have the same capacitance values at full depletion voltage (100 V before irradiation and 200 V after irradiation) as in our previous model and the appropriate strip leakage current (200 pA before irradiation and 900 nA after irradiation for 57.4 mm long strip). In this way the noise component 2 is also taken into account. By reproducing the capacitance measurements, we did not find any difference using diodes or resistors and capacitors between the implants and the back. The two models also resulted to be equivalent in concern with the simulation of signal coupling.

	57.4 mm strip length		114.8 mm strip length	
	Before irradiation	After irradiation	Before irradiation	After irradiation
Calculation				
ENC_1	989	877	1420	1197
ENC_2	11	713	15	1008
ENC_3	120	120	120	120
ENC_4	352	261	997	739
Total ENC	1056	1166	1739	1735
Simulation				
Total ENC	1039	1051	1466	1507

Table 4: Calculated and simulated noise in ENC units for 112 μm read-out pitch.

Table 4 compares the noise evaluated by the previous formulas and the noise simulated by our model. The noise for 114.8 mm strip length is much higher than that one for 57.4 mm long strips because C_{load} increases approximately linearly with the strip length. After irradiation the leakage current and the related noise (noise component 2) increase considerably. On the other hand, we measured a lower inter-strip capacitance after irradiation [2], which means that C_{load} is also lower after irradiation resulting in a lower series noise (noise components 1 and 4) after irradiation. The noise of the leakage current is almost compensated in our case by the decreasing noise due to the preamplifier and the series resistors.

It is worth noting that in p^+ on n devices an opposite behaviour is observed: the increase of the series noise after irradiation [1]. This reflects the fact that the inter-strip capacitance in a p^+ on n detector increases with irradiation.

The noise levels in the case of 224 μm read-out pitch are similar to the one of 112 μm read-out pitch: 1344 and 1432 before and after irradiation, respectively, for 114.8 mm strip length.

5 Signal-to-noise ratio

Since in our simulation the amplification of the read-out electronics can be changed arbitrarily, only the signal-to-noise ratios can be compared with the experimental data.

We compared the results of the simulation with the experimental data obtained by exposing the detector to a particle beam at a temperature of 268 K [5]. The measurements were performed with a daisy-chained detector pair (114.8 mm strip length) before irradiation and after irradiation with a fluence of $8 \cdot 10^{13}$ n/cm^2 at different bias voltages. Here we refer to the data taken at 100 V before irradiation and 200 V after irradiation, which corresponds to about 50 V above the full depletion voltages in both cases. The leakage current after the irradiation increased from 400 pA to 1.8 μA. With an external tracking system we were able to determine the impact position of the particles with a precision of 8 μm [10]. We selected events where the beam particles hit the detector close to a read-out or a non-read-out strip. If every read-out strip was connected to the read-out electronics, the particles crossing the detector close to a read-out strip induced signal mainly on one strip only; if the particles hit the detector close to a non-read-out strip the two adjacent read-out strips had signal above the threshold, with nearly equal signal amplitudes on both strips. When only every second read-out strips were connected to the read-out electronics, the events were mostly 1-strip clusters if the particle impact was close to a connected read-out or non-read-out strip, and they were mainly 2-strip clusters in case of impact close to a not connected read-out strip. The most probable values of signal amplitudes were obtained by fitting the distribution of signal amplitudes with Landau-curves [5]. The noise distribution was fitted with Gaussians. The signal-to-noise ratio was calculated as the ratio of the most probable values of the signal and noise.

	57.4 mm strip length				114.8 mm strip length			
	Before irradiation		After irradiation		Before irradiation		After irradiation	
	read-out	non-read-out	read-out	non-read-out	read-out	non-read-out	read-out	non-read-out
Calc.	19.8	18	18.2	14.6	12	11	12.3	9.8
Sim.	19.8	16.6	20	13.2	13.5	10.9	14.2	9.5
Meas.					14.2	11.1	14.7	11.5

Table 5: Comparison of the calculated, simulated and experimental signal-to-noise ratio (112 μm read-out pitch).

In table 5, we compare the calculated, simulated and measured values in the case of 112 μm read-out pitch. The calculation was made by using the charge coupling efficiencies listed in table 2, the ENC values of table 4 and assuming that the injected signal is equal to 22400 e^-.

We obtained a good agreement between the simulated and measured signal-to-noise ratio. The calculation does not take into account the resistive coupling between the detector elements. Therefore, the agreement between the calculated and measured values is worse.

The signal-to-noise ratio is lower for non-read-out strips than for read-out strips. This can be explained by the less efficient charge coupling. The coupling of non-read-out strips, and therefore S/N, is especially low after irradiation, since the inter-strip capacitance decreases with irradiation.

In the case of 224 μm read-out pitch, the signal coupling of non-read-out and not connected read-out strips is very weak, and therefore S/N is low (table 6). We cannot compare these values with the test beam results directly, since the low statistics of the data sample did not allow us to evaluate S/N separately for read-out, non-read-out and not connected read-out strips. Experimentally we have obtained only the mean S/N, which results to be 11.1 before irradiation and 8.3 after irradiation [5]. These values are comparable with the simulated ones. Infact, the experimental values can be reproduced as the mean value of the simulated ones weighted with the fraction of the pitch in which we expect signal on read-out strip (0.25), on non-read-out strip (0.5) and not connected read-out strip (0.25).

Before irradiation			After irradiation		
conn. read-out	non-read-out	not conn. read-out	conn. read-out	non-read-out	not conn. read-out
15.8	9.8	8.5	14.7	7.4	6.4

Table 6: The simulated signal-to-noise ratio in the case of 224 μm read-out pitch and 114.8 mm strip length.

6 Conclusions

A SPICE network model of silicon micro-strip detectors, which is able to reproduce the frequency dependence of the capacitance measurements, is very suitable to simulate the signal processing and noise of the detector. This model takes into account the complex R-C structure of the detector.

We obtained a good agreement between experimental and simulated signal-to-noise ratio. The simulation proved to be very useful to support the experimental data and to understand the operation of the detectors.

Acknowledgements

We would like to express our thanks to the CMS Si tracker collaboration who have stimulated this work, especially to Andrea Candelori who supported us with the circuit model of PreMux-128 and important information about the noise simulation of the preamplifier. We are also grateful to G. Sala for his technical assistance.

References

1. CMS, The Tracker Project, Technical Design Report, CERN/LHCC 98-6 CMS TDR (1998).

2. M. M. Angarano, A. Bader, D. Creanza, M. de Palma, S. My, G. Raso, P. Tempesta: Characteristics and SPICE simulation of a single-sided, n^+ on n type Si strip detector before and after neutron irradiation, CERN CMS NOTE 1998/34, accepted for publication in Nucl. Instrum. Meth. A.

3. The ATLAS Prototype Detector, SINTEF, http://www.oslo.sintef.no/ecy/7230/atlas.html.

4. Powerview 6.1, Viewlogic Systems Inc. 1997.

5. M. M. Angarano *et al.*: Test beam results of an irradiated n^+ on n type Si microstrip detector, CMS Note in preparation.

6. Zheng Li and H. W. Kraner, Nucl. Phys. B 32 (1993) 398.

7. C. Bozzi: Signal-to-Noise Evaluation for the CMS Silicon Microstrip Detectors, CERN CMS NOTE 1997/026.

8. A. Candelori, A. Paccagnella, F. Nardi, A. Bacchetta and D. Bisello: SPICE evaluation of the S/N ratio for Si microstrip detectors, Il Nuovo Cimento Vol. 109 A (1999).

9. RD2 Status report, CERN/DRDC 94-34, RD48 Status Report CERN/LHCC 97-38.

10. L. Celano *et al.*, Nucl. Instrum. Meth. A 381 (1996) 49-56.